In situ powder neutron diffraction study of non-stoichiometric phase formation during the hydrogenation† of Li_3N

Daniel J. Bull,*[a] Natalie Sorbie,[b] Gael Baldissin,[a] David Moser,[a] Mark T. F. Telling,[c] Ronald I. Smith,[c] Duncan H. Gregory[b] and D. Keith Ross[a]

Received 14th December 2010, Accepted 1st February 2011
DOI: 10.1039/c0fd00020e

The hydrogenation of Li_3N at low chemical potential has been studied *in situ* by time-of-flight powder neutron diffraction and the formation of a non-stoichiometric $Li_{4-2x}NH$ phase and Li_4NH observed. The results are interpreted in terms of a model for the reaction pathway involving the production of Li_4NH and Li_2NH, which subsequently react together to form $Li_{4-2x}NH$. Possible mechanisms for the production of Li_4NH from the hydrogenation of Li_3N are discussed.

1. Introduction

Chen *et al.* originally reported the absorption of hydrogen in Li_3N to occur *via* a reaction of stoichiometric compounds:[1]

$$Li_3N + H_2 \rightleftharpoons Li_2NH + LiH \quad (1)$$

On the basis of *in situ* neutron diffraction measurements, some of the present authors reported an alternative reaction pathway involving the suppression of LiH in the initial stages of hydrogenation, in addition to the transient formation of Li_4NH and a cubic phase with a variable lattice parameter, related to the stoichiometric imide, Li_2NH.[2] A possible reaction pathway involving Li_4NH, with the same end-members as in (1) is:

$$\begin{gathered} Li_3N + 0.5H_2 \rightarrow 0.5(Li_4NH + Li_2NH) \\ 0.5(Li_4NH + Li_2NH) + 0.5H_2 \rightarrow Li_2NH + LiH \end{gathered} \quad (2)$$

On the basis of Density Functional Theory calculations, Michel *et al.*[3] reported that this reaction pathway is marginally energetically favorable compared with reaction (1). The experimentally observed cubic phase has been denoted as quasi-imide,[2] owing to its similarity with the stoichiometric imide. The quasi-imide phase is believed to be the product of a reaction between Li_4NH and Li_2NH, forming either a non-stoichiometric single phase or an intergrowth phase. Indeed, mechanical

[a]*Materials and Physics Research Centre, University of Salford, Salford, Greater Manchester, M5 4WT, UK. E-mail: d.j.bull@salford.ac.uk; Fax: +44 161 295 5575; Tel: +44 161 295 3269*
[b]*WestCHEM, Department of Chemistry, University of Glasgow, Glasgow, G12 8QQ, UK*
[c]*ISIS Facility, Rutherford Appleton Laboratory, Harwell Science and Innovation Campus, Didcot, Oxfordshire, OX11 0QX, UK*

† We would note that neutron diffraction necessitates the use of the isotope deuterium; the term hydrogen is used in this work in a generic context.

ART ■ C0FD00020E

mixtures of Li_4NH and Li_2NH have been shown to form single phase components through solid-state diffusion,[4,5] according to:

$$(1-x)Li_4NH + xLi_2NH \rightarrow Li_{4-2x}N_{1-x}H_{1-x}(NH)_x. \quad (3)$$

The product in (3) has a mixture of the anionic species N^{3-}, H^- and $(NH)^{2-}$, giving an overall composition $Li_{4-2x}NH$. The occurrence of the quasi-imide phase has been shown to be dependent on the hydrogen chemical potential.[6] Specifically, at 250 °C, its formation appears to be suppressed for hydrogen pressures in excess of 0.5 bars. In the present work, the pressure is kept below 0.5 bars at all stages of hydrogenation.

2. Experimental

A commercially produced sample of Li_3N (Sigma Aldrich, 99%) was loaded into a custom designed pressure cell of internal volume 2 cc, with an Al_2O_3 coated vanadium window, as described in ref. 2. Neutron diffraction patterns were measured on OSIRIS[7] at the ISIS neutron facility, UK. The sample is originally observed to be a two-phase mixture of the stable α and the high-pressure β polymorphs of Li_3N; annealing the sample under vacuum at 250 °C for 2 h results in a complete conversion to the α-phase. Loading of hydrogen (deuterium) was effected at 250 °C *via* the Sieverts method, as described previously,[6] with a buffer volume of 500 cc, enabling the required molar up-take in each step to be achieved without the pressure exceeding 0.5 bars. Under these conditions, the formation of the stoichiometric Li_2NH will be precluded, at least in the initial stages of the hydrogenation reaction.[6] Diffraction patterns were collected at molar concentrations $x = \{0.1, 0.15, 0.2, 0.25, 0.3, 0.35, 0.4, 0.5, 0.67, 0.875, 1\}$, where x is the molar ratio of H_2 absorbed to the original Li_3N. For each step, data collection commenced once the rate-of-change of pressure had reached zero; an indication that the overall hydrogen content was stable. Each data set was collected for 1 h. The diffraction patterns were analysed by the Rietveld method using the GSAS software system[8] to determine the crystalline phases present, and their abundance, throughout the hydrogenation process. Structural models used in the refinement are from Niewa[9] for Li_4NH, Ohoyama *et al.*[10] for Li_2NH and Bull *et al.*[5] for $Li_{4-2x}NH$.

3. Results and discussion

Two distinct regions can be identified in the neutron diffraction data, marked by the appearance of LiH at around $x = 0.5$ in the measured patterns. Fig. 1 shows representative diffraction patterns, along with the refined structural models, in these two regions, at $x = 0.3$ and $x = 0.875$. The molar phase fractions and quasi-imide lattice parameter obtained from Rietveld refinement are shown in Fig. 2a and b. Lines in these figures are calculated from the various reaction pathways, as described below. In the initial stages of hydrogenation, for $x \sim \leq 0.5$, three phases are present in the sample – Li_3N, Li_4NH and a quasi-imide phase. The lattice parameter of the latter phase in this region exhibits some variation, shown in Fig. 2b. Above $x = 0.5$, the phase fraction of Li_4NH is observed to reduce, correlating with the formation of LiH and there is a marked change in the refined lattice parameter.

In order to interpret these results, they are compared to the reaction pathways in (1) and (2), where the phase fractions, as a function of x, can be uniquely determined; details of such a calculation are given in the appendix. From the reaction pathway in (1),

$$Li_3N + xH_2 \rightarrow (1-x)Li_3N + xLi_2NH + xLiH \qquad 0 \leq x \leq 1 \quad (4)$$

From the reaction pathways in (2):

ART ■ C0FD00020E

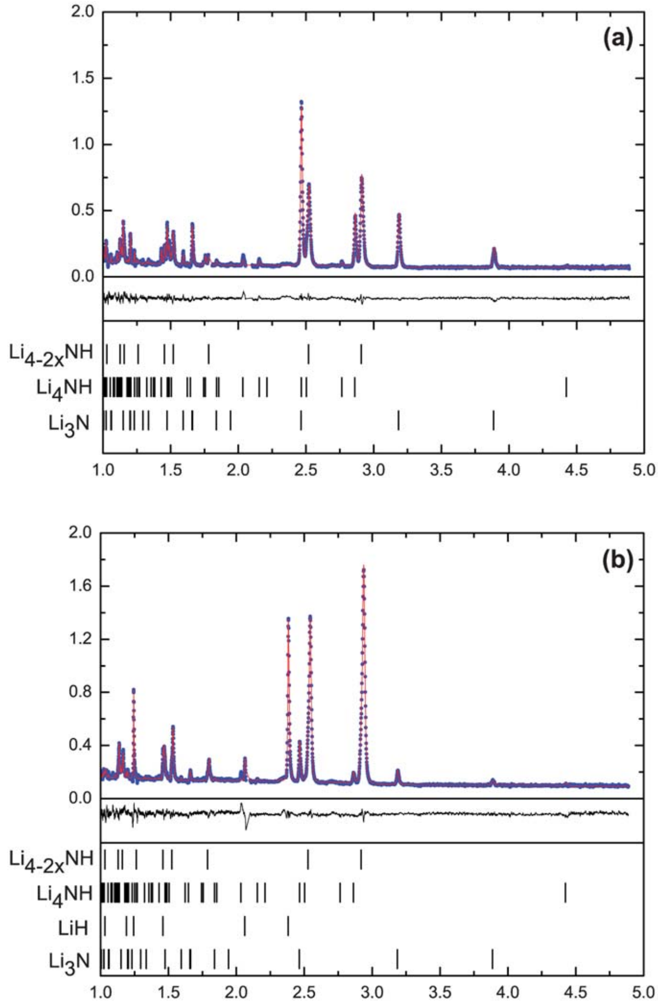

Fig. 1 Neutron powder diffraction patterns and corresponding structural refinement at 250 °C following hydrogen absorption in Li_3N at molar ratios of (a) $x = 0.3$ and (b) $x = 0.875$. The weighted-profile R-factor, R_{wp}, for the two refinements are 0.057 and 0.046, respectively.

$$Li_3N + xH_2 \rightarrow \begin{cases} (1-2x)Li_3N + xLi_4NH + xLi_2NH & 0 \le x \le 0.5 \\ (1-x)Li_4NH + xLi_2NH + (2x-1)LiH & 0.5 \le x \le 1 \end{cases} \quad (5)$$

Further, including the solid-state reaction in (3):

$$Li_3N + xH_2 \rightarrow \begin{cases} (1-2x)Li_3N + Li_3N_{0.5}H_{0.5}(NH)_{0.5} & 0 \le x \le 0.5 \\ Li_{4-2x}N_{1-x}H_{1-x}(NH)_x + (2x-1)LiH & 0.5 \le x \le 1 \end{cases} \quad (6)$$

The molar phase fractions calculated from reaction pathways in (4), (5) and (6) are shown in Fig. 3. The experimentally observed molar phase fractions for Li_3N up to $x \sim 0.3$, and for LiH correlate well with the calculated values in (5) and (6), with those for $Li_{4-2x}NH$ and Li_4NH falling somewhere between the two models, suggesting that reaction (3) is only partially completed. We would note that, since this is

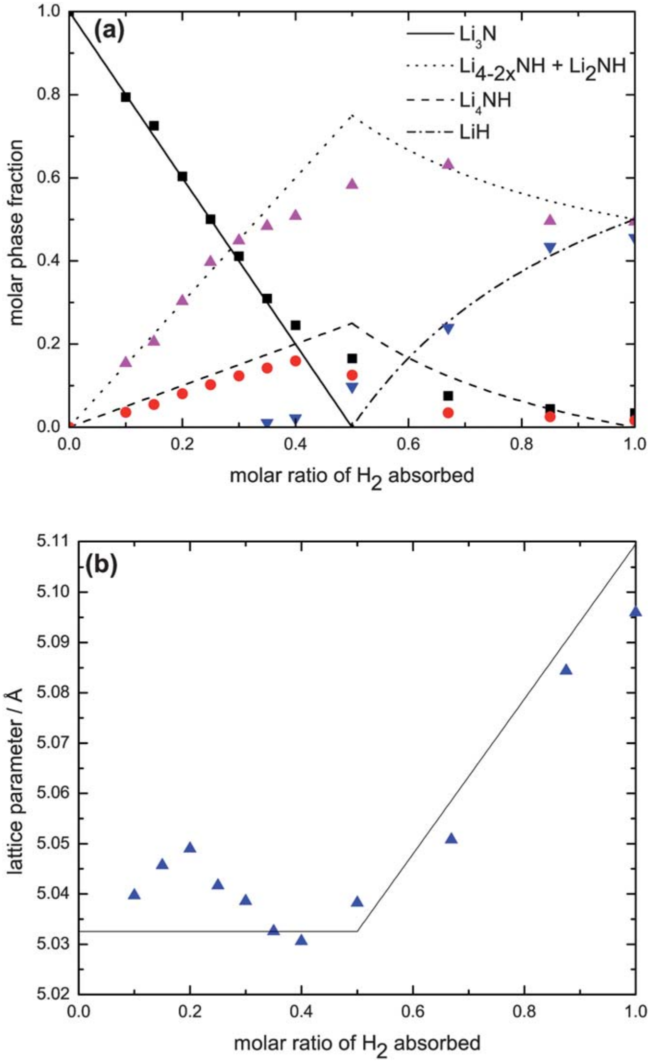

Fig. 2 Parameters determined from Rietveld refinement of neutron diffraction data from hydrogen absorption in Li_3N. (a) Molar phase fractions lines calculated from the hypothetical reaction pathway in (7), as described in the main text, and symbols representing experimentally determined values (squares – Li_3N, circles – Li_4NH, up-triangles – $Li_{4-2x}NH$ and down-triangles – LiH). (b) Lattice parameter of the cubic quasi-imide phase (symbols), $Li_{4-2x}NH$, with corresponding calculated values from (6), as described in the main text (solid line).

a solid state reaction, it does not have an effect on the hydrogen pressure. If a fraction, y, remains unreacted, the pathway can be written as:

$$\mathrm{Li_3N} + x\mathrm{H_2} \rightarrow \begin{cases} (1-2x)\mathrm{Li_3N} + y[x\mathrm{Li_4NH} + x\mathrm{Li_2NH}] + (1-y)\mathrm{Li_3NH} & 0 \leq x \leq 0.5 \\ y[(1-x)\mathrm{Li_4NH} + x\mathrm{Li_2NH}] + (1-y)\mathrm{Li_{4-2x}NH} + (2x-1)\mathrm{LiH} & 0.5 \leq x \leq 1 \end{cases} \quad (7)$$

The phase fractions from (7) with $y = 0.5$ are shown in Fig. 2a compared with the experimental data. No Li_2NH is discernable in the neutron diffraction data, hence the calculated fractions for Li_2NH have been added to that of the quasi-imide

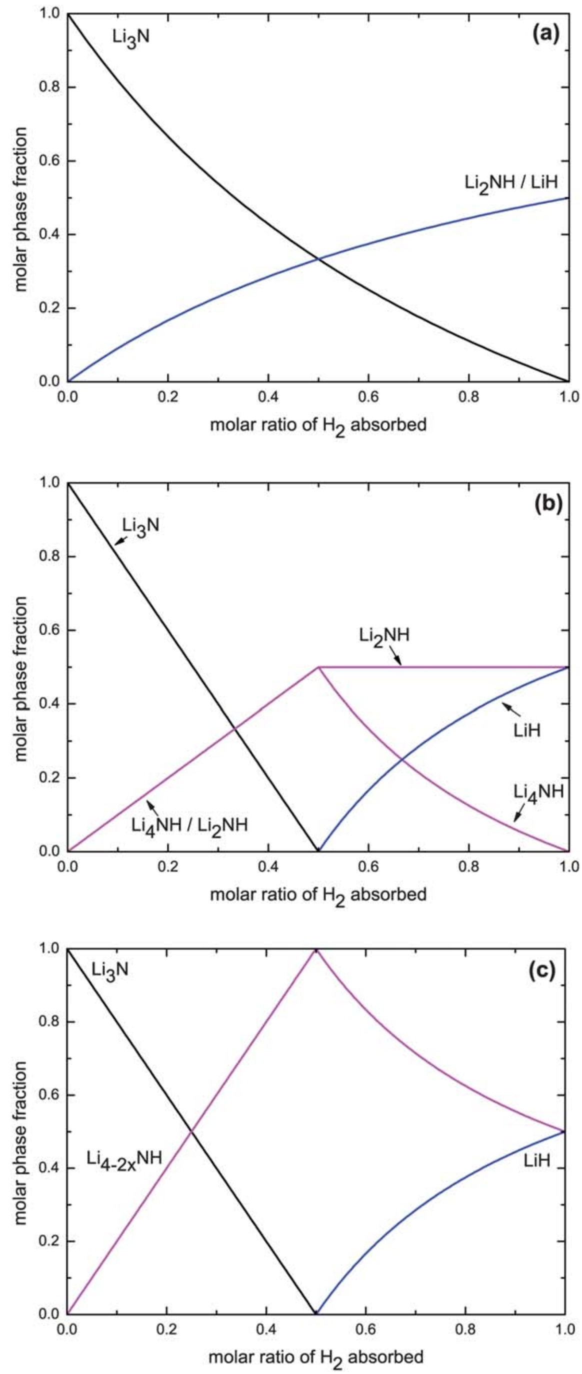

Fig. 3 Calculated molar phase fractions from (a) reaction pathway (4), (b) reaction pathways (5) and (c) reaction pathways (5) followed by the solid-state reaction (6).

phase to enable a direct comparison. The refined phase fractions are represented reasonably well across the range of x, with the exception of the proximity of $x = 0.5$. In this region, a new phase is forming, and the quasi-imide is changing its stoichiometry, so the relaxation time of the phase transitions might be expected to be large. Hence, the value of y might be expected to vary across the range of x.

The quasi-imide phase as expressed in (6) is suggestive of non-stoichiometry on the Li lattice, which is not the case in this structural model. Rather, the non-stoichiometry arises from the interchange of the anionic species, which can be made clearer by expressing the composition in relation to the stoichiometric imide as:

$$Li_2N_{\frac{1-x}{2-x}}H_{\frac{1-x}{2-x}}(NH)_{\frac{x}{2-x}}. \quad (8)$$

The variation of the quasi-imide lattice parameter with x is estimated by interpolation of data at $x = 1$ and 0.6, taken from Bull *et al.*,[5] from which a linear variation, $a = 4.9555 + 0.1541x$, is obtained. Using this in conjunction with (6) enables the variation in the lattice parameter along the reaction pathway to be determined. Up to $x = 0.5$ is compositionally invariant, and so the lattice parameter is constant. Above $x = 0.5$, there is a linear increase in the lattice parameter. As can be seen in Fig. 2b, there is a good level of agreement with the calculated and empirical values.

Whilst the exact mechanisms of hydrogenation in this system are still not clear, both the refined phase fractions and the variation in the quasi-imide lattice parameter lend weight to the reaction pathways in (2) and (3). In particular, the suppression of LiH in the initial stages of hydrogenation provides an excess of Li, which is accommodated in either the Li_4NH or $Li_{4-2x}NH$ phase. It is, therefore, of interest to consider how these phases might form. There is a wealth of literature concerning superionic conductivity in Li_3N, in particular the beneficial role of small amounts of hydrogen on ionic conductivity.[11–14] In the pure material, vacancies play a vital role in determining the ionic conductivity,[15] and so it might be expected that they are also important in the hydrogenation process. Li_3N has a layered structure comprising alternate planes of Li_2N and of Li.[16] An intrinsic Frenkel-pair defect can be introduced by the transport of a Li atom from the Li_2N layer to the Li layer:[15]

$$2[Li_3N]^0 \rightarrow [Li_2N]^- + [Li_4N]^+ \quad (9)$$

This type of mechanism would allow, in principle, the addition of heterolytically dissociated hydrogen to produce Li_2NH and Li_4NH. Wahl discusses the substitution of Li with H,[17] leading to the formation of NH^{2-} anions. The negative charge can be stabilised by the addition of Li^+ from a neighbouring cell, resulting in a vacancy in the Li_2N plane:

$$[Li_3N]^0 + [Li_2NH]^0 \rightarrow [Li_2N]^- + [Li_3NH]^+ \quad (10)$$

Of particular relevance in this mechanism is the production of the compound Li_3NH.

4. Conclusion

In situ powder neutron diffraction data from the hydrogenation of Li_3N have been presented. Rietveld profile refinement of a structural model to the data has been used to determine the relative phase fractions along the reaction pathway. The appearance of a non-stoichiometric phase, $Li_{4-2x}NH$, exhibiting a variation in lattice parameter with overall hydrogen content, has been observed. The analysis has been interpreted in terms of a reaction pathway with the transient formation of Li_4NH and Li_2NH, and the subsequent solid-state reaction to $Li_{4-2x}NH$.

ART ■ C0FD00020E

A. Calculation of reaction pathways

The reaction pathway associated with (1) can be expressed in terms of x, the ratio of moles of H_2 absorbed to moles of Li_3N:

$$Li_3N + xH_2 \rightarrow n_{Li_3N}Li_3N + n_{Li_2NH}Li_2NH + n_{LiH}LiH \quad (11)$$

where n_{Li_3N}, n_{Li_2NH} and n_{LiH} are the molar amounts of Li_3N, Li_2NH and LiH. It is possible to relate the molar amounts and the number of each component in a matrix formalism:

$$\begin{pmatrix} 3 \\ 1 \\ 2x \end{pmatrix} = \begin{pmatrix} 3 & 2 & 1 \\ 1 & 1 & 0 \\ 0 & 1 & 1 \end{pmatrix} \begin{pmatrix} n_{Li_3N} \\ n_{Li_2NH} \\ n_{LiH} \end{pmatrix} \quad (12)$$

where the column matrix on the LHS represents the amount of Li, N and H in the reactants, and the 3×3 matrix represents the amount of Li, N and H in each of the products. The molar amounts can be can be obtained by inversion of the 3×3 matrix:

$$\begin{pmatrix} n_{Li_3N} \\ n_{Li_2NH} \\ n_{LiH} \end{pmatrix} = \begin{pmatrix} 3 \\ 1 \\ 2x \end{pmatrix} \begin{pmatrix} \frac{1}{2} & -\frac{1}{2} & -\frac{1}{2} \\ -\frac{1}{2} & \frac{3}{2} & \frac{1}{2} \\ \frac{1}{2} & -\frac{3}{2} & \frac{1}{2} \end{pmatrix} = \begin{pmatrix} 1-x \\ x \\ x \end{pmatrix} \quad (13)$$

Yielding the reaction:

$$Li_3N + xH_2 \rightarrow (1-x)Li_3N + xLi_2NH + xLiH \quad (14)$$

The phase fractions are then:

$$f_{Li_3N} = \frac{1-x}{1+x} \quad (15)$$

$$f_{Li_2NH} = \frac{1}{1+x} \quad (16)$$

$$f_{LiH} = \frac{1}{1+x} \quad (17)$$

Acknowledgements

The UK Engineering and Physical Sciences Research Council for financial support. The Science and Technology Facilities Council for provision of neutron beamtime. The authors would also like to express their gratitude to Dr Eveline Weidner for her invaluable discussions.

References

1 P. Chen, Z. T. Xiong, J. Z. Luo, J. Y. Lin and K. L. Tan, *Nature*, 2002, **420**, 302–304.
2 E. Weidner, D. J. Bull, I. L. Shabalin, S. G. Keens, M. T. F. Telling and D. K. Ross, *Chem. Phys. Lett.*, 2007, **444**, 76–79.
3 K. J. Michel, A. R. Akbarzadeh and V. Ozolins, *J. Phys. Chem. C*, 2009, **113**, 14551–14558.
4 R. Marx, *Z. Anorg. Allg. Chem.*, 1997, **623**, 1912–1916.

ART ■ C0FD00020E

5 D. J. Bull, G. Baldissin, N. Sorbie, D. Moser, N. Boag, R. Smith and D. Gregory, to be published.
6 D. J. Bull, E. Weidner, I. L. Shabalin, M. T. F. Telling, C. M. Jewell, D. H. Gregory and D. K. Ross, *Phys. Chem. Chem. Phys.*, 2010, **12**, 2089–2097.
7 M. T. F. Telling and K. H. Andersen, *Phys. Chem. Chem. Phys.*, 2005, **7**, 1255–1261.
8 A. C. Larson and R. B. von Dreele, Los Alamos National Laboratory Report LAUR 86-748, 2000.
9 R. Niewa and D. A. Zherebtsov, *Z. Krist.-New. Cryst. St.*, 2002, **217**, 317–318.
10 K. Ohoyama, Y. Nakamori, S. Orimo and K. Yamada, *J. Phys. Soc. Jpn.*, 2005, **74**, 483–487.
11 A. Hooper, T. Lapp and S. Skaarup, *Mater. Res. Bull.*, 1979, **14**, 1617–1622.
12 M. Bell and R. Armstong, *J. Electroanal. Chem.*, 1981, **129**, 321–325.
13 J. Macdonald, A. Hooper and A. Lehnen, *Solid State Ionics*, 1982, **6**, 65–77.
14 T. Lapp, S. Skaarup and A. Hooper, *Solid State Ionics*, 1983, **11**, 97–103.
15 J. Sarnthein, K. Schwarz and P. Blochl, *Phys. Rev. B: Condens. Matter*, 1996, **53**, 9084–9091.
16 D. H. Gregory, *Coord. Chem. Rev.*, 2001, **215**, 301–345.
17 J. Wahl, *Solid State Commun.*, 1979, **29**, 485–490.

ART ■ C0FD00020E